# MEAN AND FLUCTUATING INTERNAL PRESSURES INDUCED BY WIND

J. D. HOLMES

James Cook University of North Queensland, Townsville, Australia

ABSTRACT

Mean and fluctuating pressures inside buildings, induced by wind, have been investigated using boundary layer wind tunnel and computer simulation techniques. Mean and r.m.s. fluctuating internal pressure coefficients were both found to be monotonic functions of the ratio of windward to leeward opening areas.

The case of a single windward opening was treated as a damped Helmholtz resonator. Inertia effects were found to produce resonance amplification in the response of the internal pressure to turbulent external pressures and to a step change in external pressure. However, these effects are unlikely to be of much practical significance except for the case of a sudden large opening occurring in a relatively rigid building.

For correct scaling of fluctuating internal pressures, wind tunnel testing should be tested at full scale wind velocities. However, it is shown that similarity can be maintained at lower wind tunnel velocities, by distorting the internal volume by a factor equal to the square of the velocity ratio.

NOMENCLATURE

| | | | |
|---|---|---|---|
| $A$ | - opening area | $p$ | - pressure |
| $b$ | - breadth of opening | $p_0$ | - atmospheric (static) pressure |
| $c$ | - speed of sound | $q$ | - dynamic pressure |
| $C_p$ | - pressure coefficient | $Q$ | - volume rate of flow |
| $C_y^p, C_z$ | - decay constants for external pressure co-spectra (Eqn. 10) | $r$ | - $\ell_e/\sqrt{A}$ |
| $F_u$ | - empirical factor in E.S.D.U. expression for turbulence intensity (Fig. 1) | $S(n)$ | - auto-spectral density |
| $h$ | - (1) eaves height of building (2) height of opening (Eqn.10) | $t$ | - time |
| $I_u$ | - longitudinal turbulence intensity | $u$ | - longitudinal velocity component |
| $k^u$ | - orifice discharge coefficient | $V_0$ | - internal volume |
| $\ell_e$ | - effective length of air "slug" | $x$ | - displacement of air slug |
| $n$ | - (1) polytropic exponent (2) frequency | $y$ | - lateral displacement |
| $n_0$ | - Helmholtz resonance frequency | $z$ | - height |
| | | $z_0$ | - roughness length (Fig. 1) |
| | | $z_r$ | - reference height (Fig. 1) |
| | | $\Delta$ | - change |
| | | $\lambda_u$ | - peak wave length of longitudinal velocity spectrum |

$\mu$ - dynamic viscosity
$\pi_j$ - non-dimensional group
$\rho$ - air density
$\tau$ - equilibrium time
$\chi^2$ - aerodynamic admittance
Subscripts:
e - external
i - internal
L - leeward
W - windward
m - model scale
f - full scale
Superscripts:
$\bar{}$ - mean value
' - fluctuating value
* - non-dimensional

## 1. INTRODUCTION

Internal pressures induced by wind on buildings have traditionally received much less attention than have external pressures. This is the case despite the fact that, for low-rise buildings in particular, the internal pressure loading may form a high proportion of total design wind loading on both structure and cladding. During Cyclone Tracy in Darwin, Australia, for example, a high proportion of roof failures on domestic buildings were believed to have been preceded by window failure on the windward side of the building, resulting in high internal positive pressures combining with roof suctions [Walker(1)].

The relationship between *mean* internal pressures and the relative size of windward and leeward wall openings has been understood for some time [Euteneuer(2), Van Koten(3), Newberry and Eaton(4), Liu(5)], and is reflected in the coefficients of internal pressure specified in wind loading codes [e.g. S.A.A.(6)].

Euteneuer(7) derived an expression for the "response time" of the pressure inside a low-rise building to a step change in external pressure such as that caused by the sudden failure of a window; Vickery(8) and Liu(9) later derived similar expressions. Jancauskas and Sharp(10) carried out some boundary layer wind tunnel measurements in which a window failure was simulated, and the change in lift force on the roof of a 1/100 scale house model was measured. Jancauskas and Sharp also measured mean and fluctuating internal pressures for a range of windward to leeward opening ratios. Kramer, Gerhardt and Scherer(11) carried out wind tunnel measurements of response time and attributed differences from theoretical values to the effect of inertia forces.

In the present paper, a study of internal pressures in low-rise buildings, with both windward and leeward wall openings, using boundary layer wind tunnel and numerical simulation techniques, is described. The case of a single windward wall opening is treated in some detail: the effect of inertia forces, previously neglected, on the "response time" to a step change in external pressure is examined by means of numerical simulation. The fluctuating internal pressure resulting from external pressure fluctuations, due to wind turbulence, is studied using both wind tunnel and numerical simulation methods.

Although many of the results are applicable to all types of buildings, the work is mainly directed towards domestic houses and other low-rise buildings, and forms part of a research study sponsored by the Australian Housing Research Council.

This paper is a shortened version of a report [Holmes(12)], in which more detail of the theory and experimental methods is included; design applications are also discussed.

## 2. THEORY

### 2.1 Mean Pressures

The mean internal pressure coefficient inside a building with total areas of wind-

ward openings, $A_W$, and leeward openings $A_L$, can readily be derived by assuming standard orifice flow relationships in and out of the openings and considering mass conservation(3), (5), (12):

$$\overline{C_{p_i}} = \frac{\bar{p}_i - p_0}{q} = \frac{\bar{C}_{p_W}}{1 + (\frac{A_L}{A_W})^2} + \frac{\bar{C}_{p_L}}{1 + (\frac{A_W}{A_L})^2} \qquad (1)$$

where $p_0$ is the reference static (atmospheric) pressure and $q = \frac{1}{2}\rho\bar{u}^2$, is the reference dynamic pressure. $\bar{C}_{p_W}$, $\bar{C}_{p_L}$ are the external pressure coefficients at the windward and leeward openings, respectively.

## 2.2 Single Windward Opening

The case of a single windward opening is normally the critical design case for low-rise buildings and deserves special attention. The mean internal pressure coefficient, from equation (1), is equal to the mean external pressure coefficient. However, when a building is immersed in a turbulent boundary layer flow such as that characteristic of the earth's boundary layer in strong winds, the external pressure will be fluctuating or turbulent, especially for low-rise buildings, and the internal pressure will respond in some way to these fluctuations. Since there is only a single opening, flow into the building resulting from an increase in external pressure will cause an increase in density of the air within the internal volume; this, in turn, causes an increase in internal pressure. The pressure changes due to wind *relative to atmospheric pressure* are small, and the *relative* density changes are of the same order. These density changes can be maintained by only relatively small mass flows in and out of the building and the internal pressure can therefore be expected to respond fairly rapidly to external pressure changes, except for the case of a very small opening size.

It is useful, first, to carry out a dimensional analysis to establish the non-dimensional groups involved.

### 2.2.1 Dimensional analysis

From dimensional analysis the fluctuating internal pressure coefficient, $C_{p_i}'$ can be written:

$$C_{p_i}' = \frac{p_i - p_0}{\frac{1}{2}\rho\bar{u}^2} = F(\pi_1, \pi_2, \pi_3, \pi_4, \pi_5) \qquad (2)$$

where $\pi_1 = \frac{A^{3/2}}{V_0}$ ; $\pi_2 = \frac{p_0}{\frac{1}{2}\rho\bar{u}^2}$ ; $\pi_3 = \frac{\rho\bar{u}\sqrt{A}}{\mu}$ (Reynolds Number)

$\pi_4 = \frac{\sqrt{\overline{u'^2}}}{\bar{u}}$ (turbulence intensity); $\pi_5 = \frac{\lambda_u}{\sqrt{A}}$

where $\mu$ is viscosity

$\bar{u}$ is the mean velocity of the stagnation flow

$\sqrt{\overline{u'^2}}$ is the root-mean-square longitudinal turbulence component

$\lambda_u$ is the peak wave length of the longitudinal turbulence spectrum i.e. a measure of turbulence scale

$\pi_2$, the ratio of atmospheric pressure to the reference dynamic pressure, is a parameter closely related to Mach Number. The significance of this parameter remains to be established, but establishing its importance is relevant to wind tunnel testing since equality with values for full scale design cases is normally not possible in conventional boundary layer wind tunnels. The Reynolds Number, $\pi_3$, is not likely to be a significant parameter except for small opening areas, A.

2.2.2 Response time

The case of the response of the internal pressure to a sudden external pressure increase, such as that caused by a sudden window failure, has been considered previously [Euteneur(7), Vickery(8) and Liu(9)].

The conservation of mass equation can be written in this case:

Rate of mass flow in = Increase in internal mass of air

$$\rho_i Q = \left(\frac{d\rho_i}{dt}\right) V_0 \qquad \text{——————} \quad (3)$$

Assuming a polytropic law relating pressure and density:

$$\text{i.e. } \frac{p_i}{\rho_i^n} = \text{constant} \qquad \text{——————} \quad (4)$$

and for flow through the orifice:

$$Q = k A \sqrt{\frac{2(p_e - p_i)}{\rho}}, \qquad \text{——————} \quad (5)$$

it can be shown that the equilibrium time when the internal pressure becomes equal to the internal pressure is given by:

$$\tau = \frac{\rho V_0 \bar{u}}{nkAp_0} \sqrt{Cp_e - Cp_{i_0}} \qquad \text{——————} \quad (6)$$

where $Cp_{i_0}$ is the initial value of $Cp_i$

2.2.3 Helmholtz resonator model

The theoretical basis of the computer simulation models used in this paper is now described. The orifice flow and polytropic pressure-density relationship used in the previous section are retained, but in addition, the inertia effects of the air moving in and out of the opening are included. The case is, in fact, a special case of a "Helmholtz resonator" well known in acoustics [e.g. Rayleigh(13), Malecki(14)].

A "slug" of air can be considered to be moving in and out of the opening in response to the external pressure changes.

A differential equation for the motion of this mass of air can be written:

$$\rho A \ell_e \ddot{x} + \frac{\rho A}{2k^2} \dot{x}|\dot{x}| + \frac{np_0 A^2}{V_0} x = \Delta p_e A \qquad \text{——————} \quad (7)$$

This is the differential equation of a single degree of freedom dynamic system with non-linear (square law) damping. The mass of the "slug" of air is $\rho A \ell_e$, where $\ell_e$ is the effective length of the slug. $\ell_e$ can be taken to be $\sqrt{\pi A}/4$. this is strictly correct for circular openings only, but is a good approximation for rectangular openings of low aspect ratio [Malecki(14)].

The "stiffness" is the resistance of the internal pressure to unit deflection of the "slug". The damping force follows from the turbulent flow equation(5).

The undamped resonant frequency is:

$$n_0 = \frac{\omega_0}{2\pi} = \frac{1}{2\pi}\sqrt{\frac{nAp_0}{\rho \ell_e V_0}}$$

$$= \frac{cA^{1/2}}{2^{1/2}\pi^{5/4} V_0^{1/2}} \qquad (8)$$

where $c = \sqrt{\frac{np_0}{\rho}}$ is the speed of sound

Equation (8) is a well-known formula for the Helmholtz resonance frequency [Rayleigh(13), p. 187].

Equation (7) can be written with $C_{p_i}$ as the dependent variable:

$$\frac{p\ell_e V_0}{np_0} \ddot{C}_{p_i} + \frac{\rho V_0^2 q}{2k^2 n^2 A p_0^2} \dot{C}_{p_i} |\dot{C}_{p_i}| + A.C_{p_i} = A.C_{p_e} \qquad (9)$$

Equation (9) should be valid for the case of a fluctuating external pressure coefficient $Cp_e$ induced by wind turbulence, provided that the parameter $\lambda_u / \sqrt{A}$ ($\pi_5$ in section 2.2.1) is large, i.e. if the opening dimensions are small in comparison with the scale of turbulence. Equation (9) was used as the basis of the computer simulation method described in this paper. The equation is solved for the time-varying internal pressure coefficient $C_{p_i}(t)$ for a specified external pressure variation $C_{p_e}(t)$.

## 3. INVESTIGATION TECHNIQUES

### 3.1 Boundary Layer Wind Tunnel Measurements

The wind tunnel measurements described in this paper were carried out on a $^1/_{50}$ scale model of a two storey house in the James Cook University boundary layer wind tunnel; the latter has been described in detail elsewhere [Holmes(15)]. A rural atmospheric boundary layer at the scale of $^1/_{50}$ was simulated by placing a 300 mm high plain fence or barrier at the start of the 13.5 m long test section followed by floor roughness consisting of carpet. This simulation method has been used for a number of studies of external wind pressures on house models carried out in this tunnel [Holmes and Best(16,17,18), and Best and Holmes(19)]. Profiles of mean velocity and turbulence intensity are shown in Figure 1 and compared with E.S.D.U.(20) data. The turbulence scale as indicated by the longitudinal turbulence spectrum is approximately half that suggested by the E.S.D.U. data for the scale of $^1/_{50}$(12).

The house model is shown in Figure 2, and was specially constructed to enable pressures at taps vented to the internal volume, to be measured, as well as at external taps. Pressure tubing connecting the external taps to the pressure transducer beneath the wind tunnel turntable, was brought in between double side walls giving a clear internal space. A previous study [Munarin(21)] had shown that the internal pressures were substantially uniform throughout the internal volume and for most of the tests described in this paper, a pressure transducer (Setra 237) was connected by a 6 mm hole to a single pressure tap on the floor of the model. The model was made from "perspex", and the external pressure taps consisted of short lengths of stainless steel tubing of about 1 mm internal diameter. A number of interchangeable panels with openings of various sizes were made to fit open sections located centrally in the front and rear walls. This enabled the windward and leeward open areas $A_W$, $A_L$ to be varied. The maximum open area obtainable was approximately 22% of the total wall surface area.

The reference dynamic pressure was obtained by measuring the free stream mean velocity $\bar{u}_h$, at a height equal to the eaves height of a building using a linearised hot-film anemometer system (T.S.I. 1054B). The reference position was about 500 mm to the side of the model centre and slightly upwind. The static pressure reference, $p_0$, was derived from a pitot-static tube mounted near the top of the wind tunnel. In a separate test, the static pressure at the reference (eaves) height was obtained and a small correction was applied to the results.

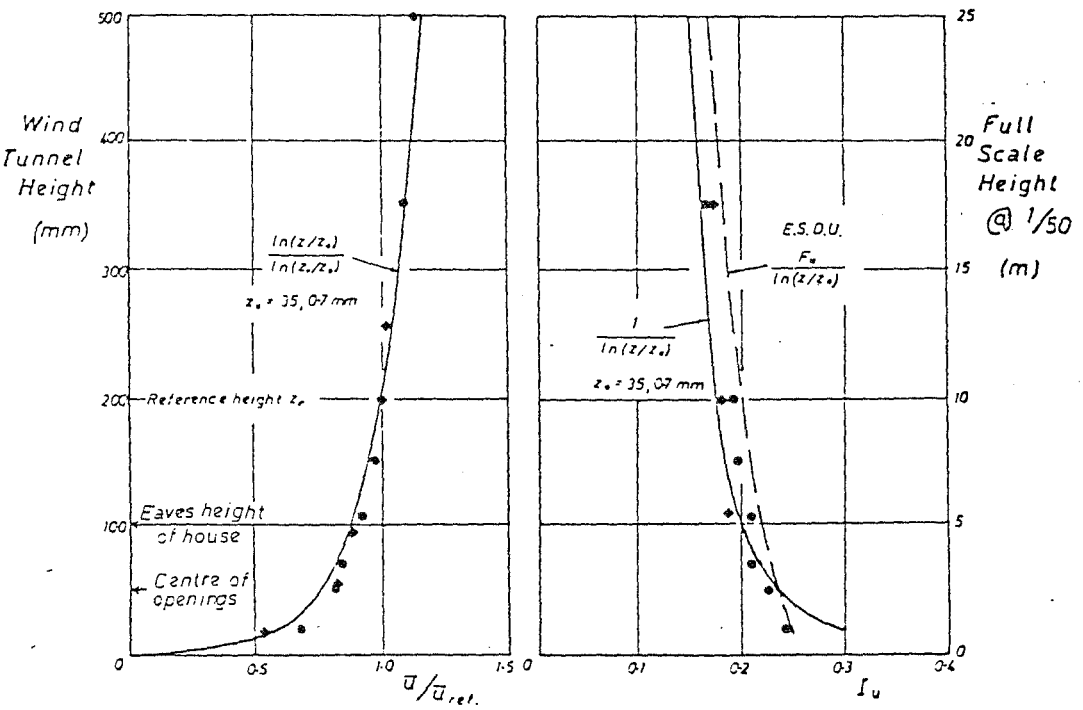


Figure 1. Wind tunnel mean velocity and turbulence intensity profiles

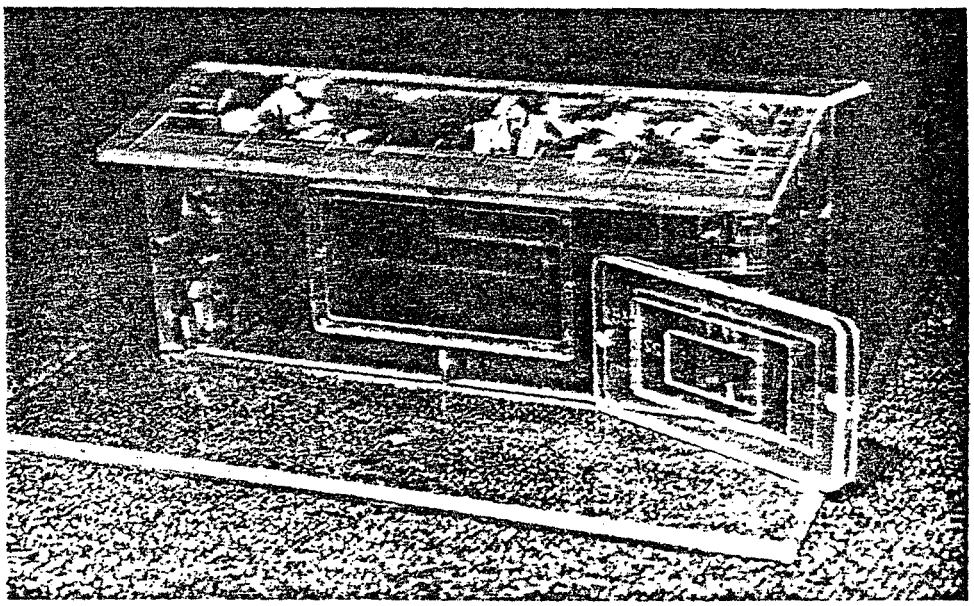

Figure 2. 1/50 scale house model

### 3.2 Computer Simulation

"Records" of external stagnation pressure representative of that on buildings in a turbulent atmospheric boundary layer were computed from simulated wind velocity records generated by the Inverse Fast Fourier transform technique [Holmes(22)]. The generation procedure incorporated a von Karman-Harris spectral model in which the length scale, $\lambda_u$, could be varied at will.

The records so generated became the "forcing function" on the right hand side of equation (9) for the single windward opening case. The equation was solved for the internal pressure variation using the lumped-impulse or central-difference method commonly used in structural dynamics [e.g. Biggs(23)].

An optional filter was incorporated to allow for the effective pressure reduction (aerodynamic admittance) over the windward opening. This filter took the form:

$$\chi^2(n) = \int_0^b\int_0^b\int_0^h\int_0^h \exp\{-\frac{n}{\bar{u}}[C_y^2(y_1 - y_2)^2 + C_z^2(z_1 - z_2)^2]^{\frac{1}{2}}\}dy_1dy_2dz_1dz_2$$

$$= \frac{4}{b^2h^2}\int_0^b\int_0^h (b-y)(h-z)\exp\{\frac{-n}{\bar{u}}[C_y^2y^2 + C_z^2z^2]^{\frac{1}{2}}\}\,dy\,dz$$

$$= 4\int_0^1\int_0^1 (1-\frac{y}{b})(1-\frac{z}{h})\exp\{\frac{-n}{\bar{u}}[C_y^2y^2 + C_z^2z^2]^{\frac{1}{2}}\}\,d(\frac{y}{b})\,d(\frac{z}{h}) \qquad \text{(10)}$$

where b, h are the opening breadth and height respectively.
The reduction to a double integral is after Bearman(24). This filter attenuated the external pressure fluctuations, the attenuation being larger for high frequencies and for large opening sizes. The constants $C_y$, $C_z$ were derived from wind tunnel tests.

## 4. RESULTS

### 4.1 Mean Internal Pressures

The mean internal pressure coefficient for a range of windward and leeward opening sizes obtained from the wind tunnel experiments is shown in Figure 3. Values obtained previously by Munarin(21) by averaging 20 second (wind tunnel time) mean values from each of the 19 individual internal pressure taps on the model are shown, as well as those from the present study, in which an ensemble average of 27 separate runs from the single floor pressure tap was calculated.

Equation (1), with appropriate values of external mean pressure coefficients, agrees well with measured data for windward opening areas greater than about 5% of the total windward wall surface area. However for the single windward opening case, there is a reduction in mean internal pressure with decreasing area, for smaller opening areas. This may be due to the effects of leakage on the leeward sides of the model becoming important.

### 4.2 Internal Pressure Fluctuations

Figure 4 is the corresponding plot to Figure 3 for the r.m.s. fluctuating internal pressure coefficient. Again a steady increase occurs with increasing $A_W/A_L$ ratio, and for opening areas over about 5% of the windward surface it is insensitive to changes in opening area. For non-zero leeward opening areas, the internal fluctuating pressure depends on the fluctuating external pressure on the leeward wall, as well as that on the windward side. The leeward external pressure fluctuations are markedly less in magnitude than the windward pressure fluctuations, and this adequately explains the reduction in internal pressure fluctuations with increasing leeward area, $A_L$.

For the single windward opening case, as is clear from sections 2.2.1 and 2.2.3,

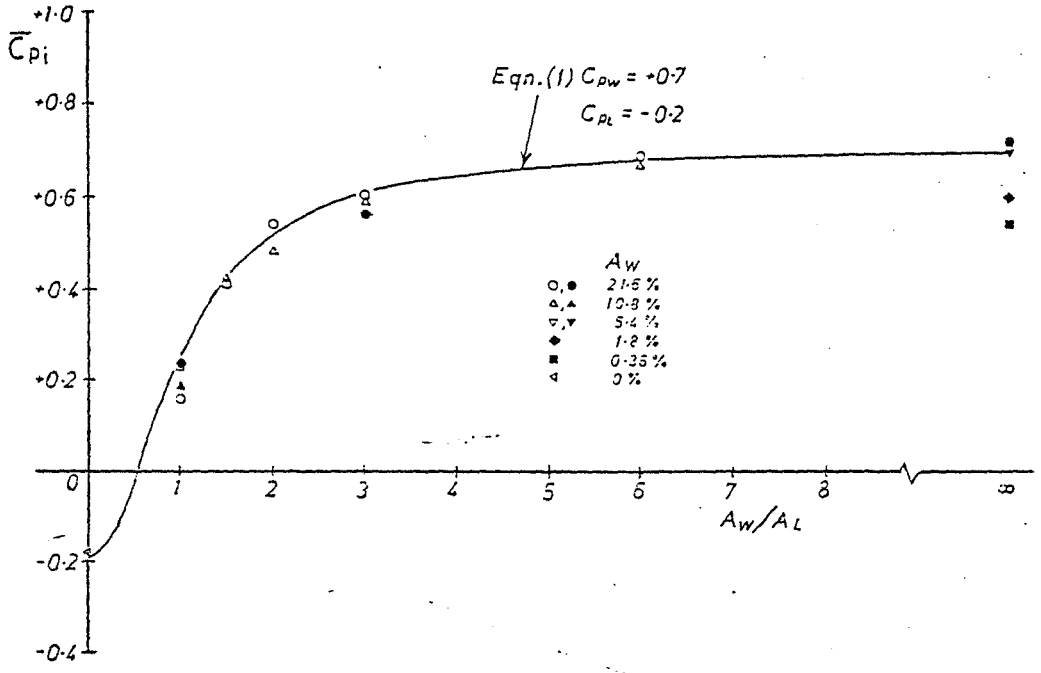


Figure 3. Mean internal pressure coefficient versus $A_W/A_L$
(Open symbols - averages over pressure taps
Solid symbols - ensemble averages for single floor tap).

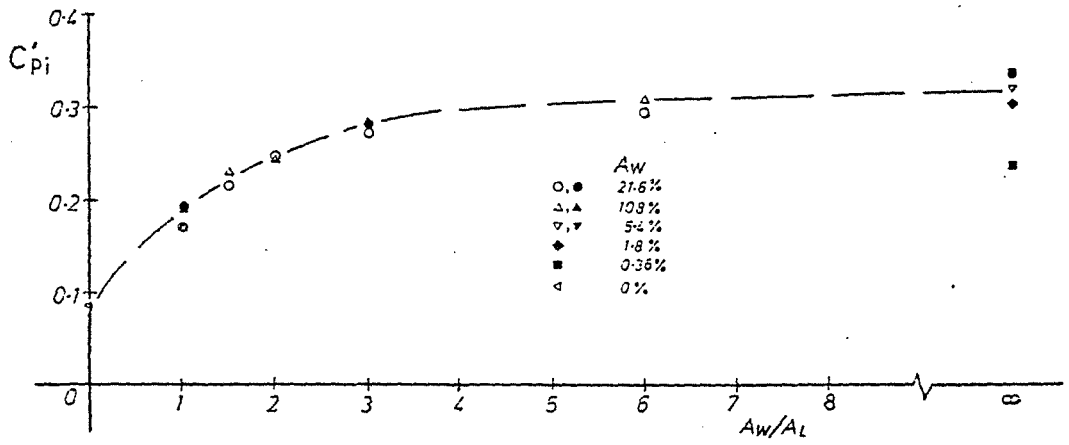


Figure 4. R.m.s. fluctuating internal pressure coefficient versus $A_W/A_L$
(Open symbols - averages over pressure taps
Solid symbols - ensemble averages for single floor tap)

the internal fluctuating pressure coefficient depends on the internal volume, $V_0$, as well as the windward area, $A_W$, i.e. on the ratio $A_W^{3/2}/V_0$. It is clear from Figure 4, for the house model, that a reduction in $A_W$, for $A_W/A_L$ equal to infinity, generally causes a reduction in the internal r.m.s. pressure coefficient.

Figures 5 to 8 show spectra estimates of the internal pressure fluctuations from the house model, for the single windward opening case, for four different values of the opening area, $A_W$. Also shown are the corresponding spectra estimates obtained from the computer simulated data. Parts of the recorded and simulated data, corresponding to Figure 6, are shown in Figure 9.

The measured and simulated data clearly show resonant peaks occurring at frequencies close to those calculated from equation (8). In agreement with this equation, the resonant frequencies increase with the opening area. In addition, the height of the peaks increases and the width decreases with increasing opening area, indicating lower damping; this again is consistent with the damping term in equation (9). The small resonant effects are apparent in the recorded and simulated data (Figure 9).

For the computer simulations, the aerodynamic admittance filter (equation (10)) was applied, using values for the constants $C_y$ and $C_z$ of 7 and 3 respectively. These were obtained by measuring the co-spectra for external pressure fluctuations on the front wall of the model with the windward opening sealed and fitting exponential decay functions, appropriate to equation (10). However, no account of the turbulence distortion effects which tend to attenuate the pressure fluctuations at high frequencies [e.g. Bearman(25), Holmes(26)] was taken. This probably partly explains the overestimates in the simulated data of the internal pressure fluctuations at frequencies below the resonant frequency for the lower windward areas (Figures 5 and 6). The leeward leakage mentioned previously may also contribute to this.

The polytropic exponent, n, is 1.0 for isothermal and 1.4 for adiabatic conditions; an intermediate value of 1.2 was used in the simulations. This was vindicated by the good agreement between the computed and measured resonant frequencies. The orifice discharge coefficient, k, is about 0.6 under steady flow conditions [Pankhurst and Holder(27)], but is likely to differ considerably from this under highly fluctuating and reversed flow conditions, as in the present case. A value of 0.15 gave resonant peaks on the simulated spectra in quite good agreement with the measured data, although a larger value may be more appropriate for smaller openings.

Although the resonant peaks on the spectra are quite marked, their contribution to the total variance is small as the frequencies are high in comparison with those of the external 'forcing' pressure fluctuations. More significant effects appear to be those of the aerodynamic admittance and turbulence distortion effects described above. Values of r.m.s. fluctuating pressure coefficients corresponding to the spectra in Figures 5 to 8 are given in Table 1.

All the results discussed previously were for a mean velocity of about 10 m/s at the eaves height of the building, and this velocity applies to both full-and model-scale. Thus the value of the $p_0/\frac{1}{2}\rho\bar{u}^2$ ($\pi_2$ in section 2.2.1) was about 1670. The effect of increasing the mean velocity is to move the resonance wave number downwards towards the main peak of the pressure spectrum, but the damping is also increased as is clear from equation (9). (Figure 7)

### 4.3 Response to a Step Change in External Pressure

The same computer program used to solve equation (9), for the simulated turbulent pressures, was also used to illustrate the effect of inertia terms on the response

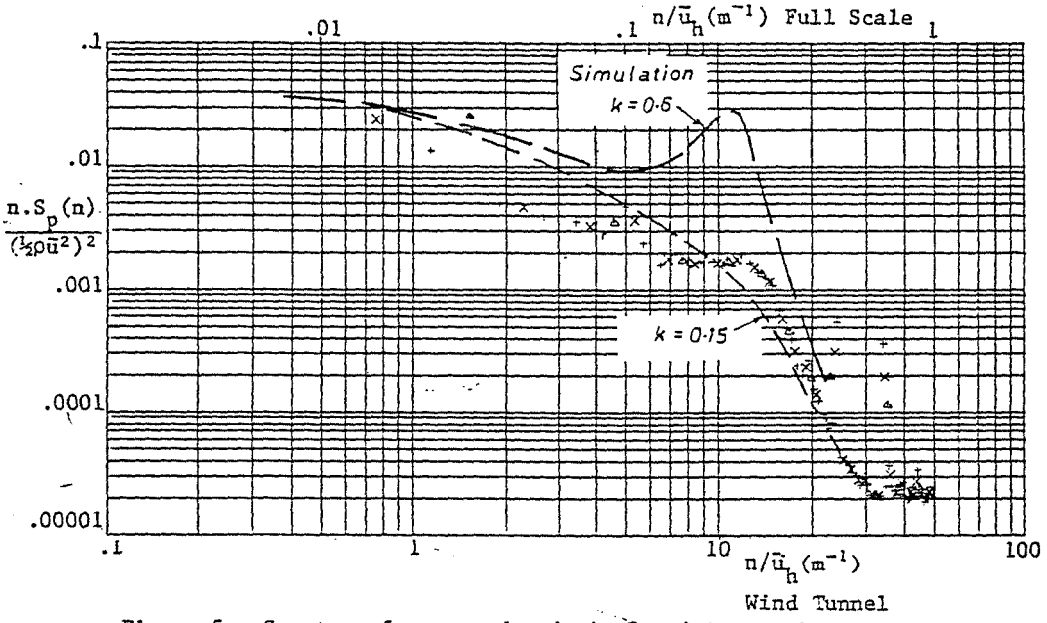


Figure 5. Spectra of measured and simulated internal pressure fluctuations. $A_w^{3/2}/V_0 = .00044$. $\bar{u}_h \simeq 10$ m/s.

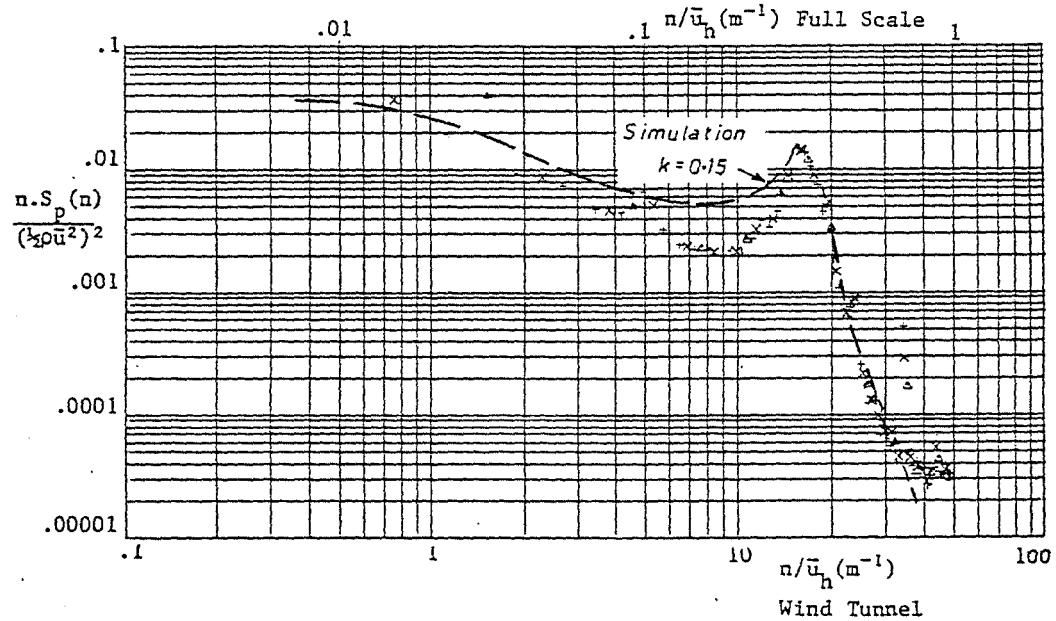


Figure 6. Spectra of measured and simulated internal pressure fluctuations. $A_w^{3/2}/V_0 = .0050$. $\bar{u}_h \simeq 10$ m/s.

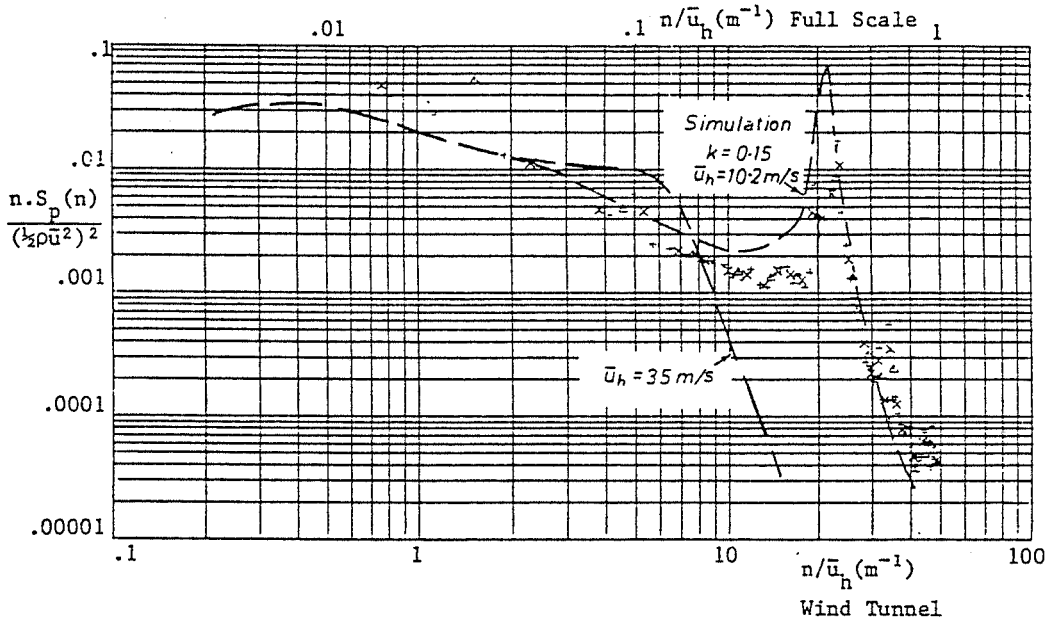


Figure 7. Spectra of measured and simulated internal pressure fluctuations. $A_W^{3/2}/V_0$ = .026.

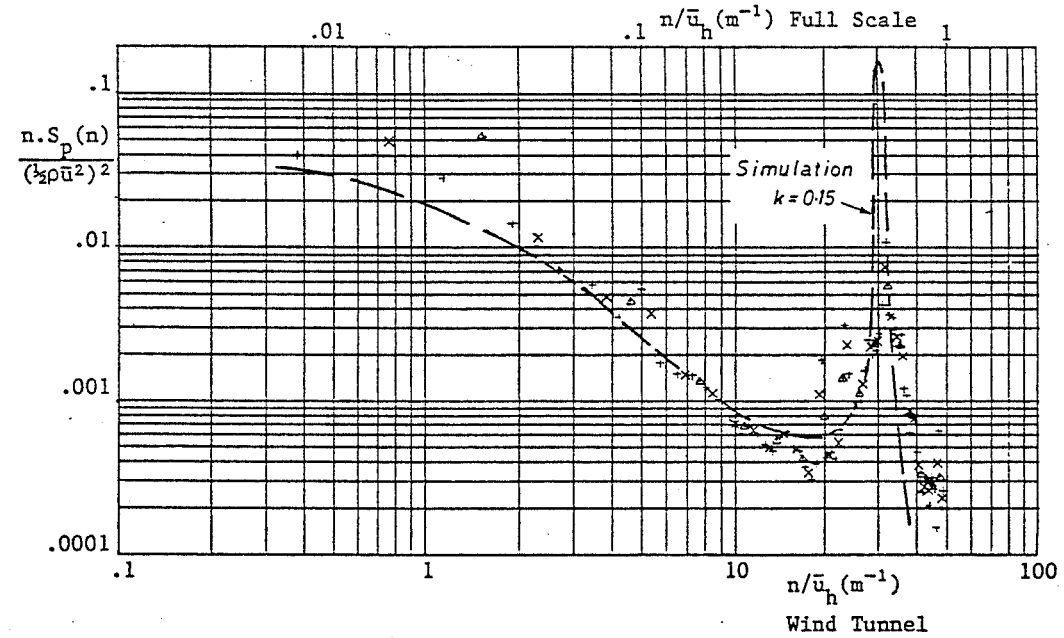


Figure 8. Spectra of measured and simulated internal pressure fluctuations. $A_W^{3/2}/V_0$ = .21. $\bar{u}_h$ ≈ 10 m/s.

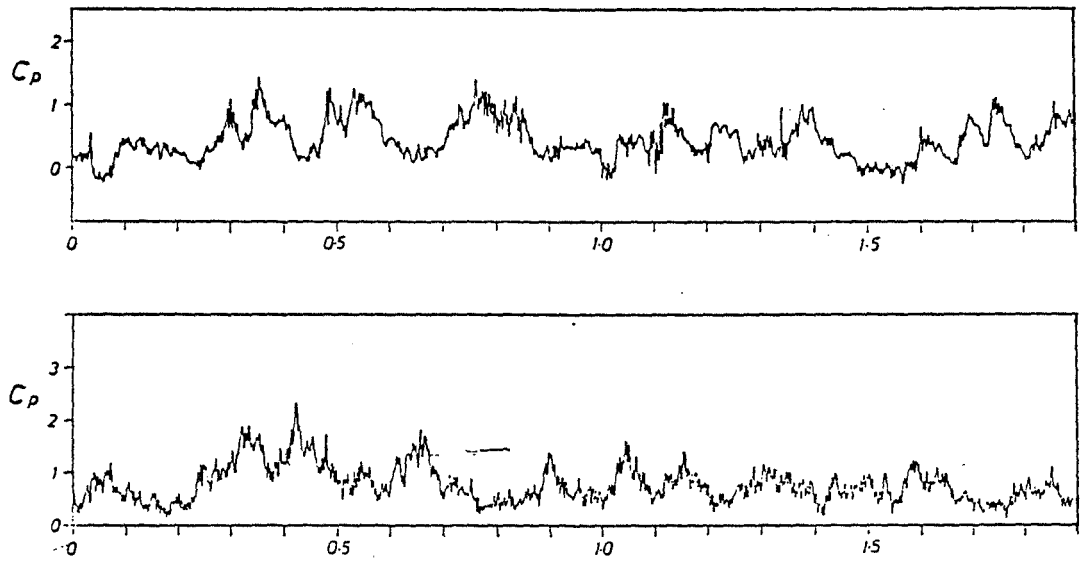


Figure 9. Measured (above) and simulated (below) records of internal pressure fluctuations. $A_W^{3/2}/V_0 = .0050$. $\bar{u}_h \approx 10$ m/s.

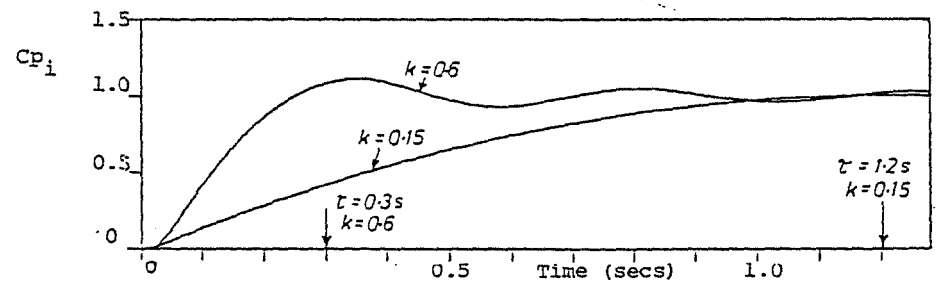


Figure 10. Response to a step change in external pressure $V_0 = 600$ m$^3$. $A_W = 1$ m$^2$. $\bar{u} = 30$ m/s.

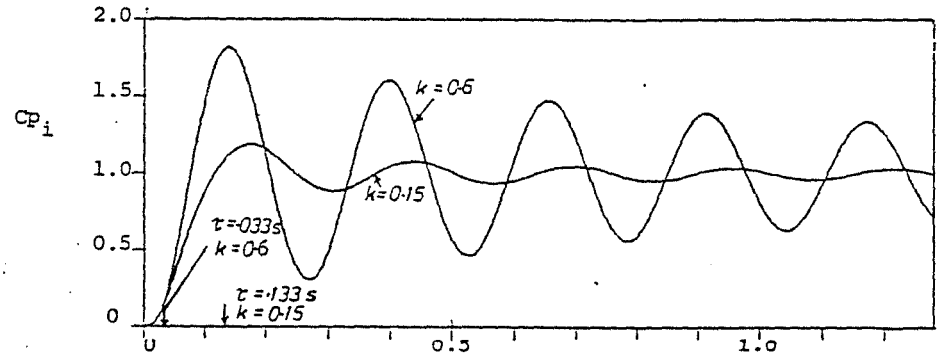


Figure 11. Response to a step change in external pressure $V_0 = 600$ m$^3$. $A_W = 9$ m$^2$. $\bar{u} = 30$ m/s.

TABLE 1. $C\acute{p}_i$ from wind tunnel measurements and simulated data for $A_W/A_L = \infty$

| $A_W^{3/2}/V_0$ | $Cp_i$ | |
|---|---|---|
| | Measured* | Simulated (k = 0.15) |
| .00044 | .238 | .326 |
| .0050 | .303 | .336 |
| .026 | .338 | .339 |
| .21 | .337 | .330 |

* ensemble average for 27 separate runs

of an internal volume to a sudden change in external pressure.

Figures 10 and 11 show the response of an internal volume of 600 $m^3$ to a step increase in external pressure coefficient from zero to 1.0; a velocity of 30 m/s, and opening areas of 1 $m^2$ and 9 $m^2$ were considered. These could represent window and door failures in a small industrial building [the 1 $m^2$ area case was used as an example by Liu(9)]. A value of orifice coefficient, k, of 0.6 might be appropriate in the initial stages when the flow is all in one direction, but if oscillations occur then, from the previous section, it appears that a lower value is applicable. Calculations were done with values of 0.6 and 0.15 for k, and the results of both cases are shown in Figures 10 and 11. Values of the equilibrium time, $\tau$, calculated from equation (6), in which inertia effects are ignored, are also shown.

Despite the doubt about the orifice coefficient, it is apparent that inertia effects are significant in the case of the larger opening when the damping term in equation (9) is much lower. This is, at least qualitatively, in agreement with the wind tunnel measurements of Kramer, Gerhardt and Scherer(11). It should be noted, however, that the effect of building flexibility has not been considered in the analysis; this is likely, in real buildings, to have a significant effect by increasing damping and reducing 'overshoot' and oscillation effects. Vickery(8), in fact, treated this effect in his consideration of response time by assuming an effective atmospheric pressure $p_0'$ given by the actual pressure $p_0$ minus a bulk modulus for the building. This procedure could easily be incorporated in the computation procedure described above, provided realistic values of bulk modulus could be established.

## 5. INTERNAL VOLUME DISTORTION

As discussed in section 2.2.1, the non-dimensional parameter $\pi_2$ ($= p_0/\frac{1}{2}\rho\bar{u}^2$) will not have the same value in full and model scales, unless the wind tunnel tests are carried out at full scale design wind velocities. Normally this is not possible and, typically, wind tunnel velocities are about one third of full scale values. The effect of this incorrect scaling was mentioned in section 4.2, and illustrated in Figure 7. For small internal volumes typical of houses and smaller industrial buildings, the effect on the r.m.s. internal pressure due to incorrect velocity scaling is small. For the case shown in Figure 7, the simulation results indicated a reduction in $C\acute{p}_i$ of only about 4% due to the increase in mean velocity. However for internal volumes characteristic of larger industrial buildings (5-10,000 $m^3$ in full scale), the computer simulation indicated somewhat larger reductions of 15-20% in r.m.s. internal pressure when the mean velocity was increased from 10 to 30 m/s.

It appears to be possible to simulate the effect of higher wind velocities in wind tunnel tests by introducing internal volume distortion, at least for the single windward opening case. This may be seen by writing equation (9) in the following non-dimensional form:

$$\left(\frac{r}{n}\right)\frac{2}{\pi_1\pi_2\pi_5^2}\frac{d^2Cp_i}{dt^{*2}} + \left(\frac{1}{k^2n^2}\right)\frac{1}{\pi_1^2\pi_2^2\pi_5^2}\frac{dCp_i}{dt^*}\left|\frac{dCp_i}{dt^*}\right| + Cp_i = Cp_e \qquad (11)$$

where $\ell_e$ has been written as $r\sqrt{A}$ and t* is a non-dimensional time equal to $\frac{t\bar{u}}{\lambda_u}$

In this equation, the product $\pi_1\pi_2$ is equal to, and can be replaced by a single non-dimensional parameter, $\pi_{12}$ equal to: $\dfrac{2A^{3/2}p_0}{\rho(\bar{u}^2V_0)}$

It should be noted that $\bar{u}$ and $V_0$ only occur together in equations (9) or (11) as a product, $\bar{u}^2V_0$. Thus, equality of $\pi_{12}$ can be maintained by ensuring that:

$$\frac{[\bar{u}^2V_0]_m}{[\bar{u}^2V_0]_f} = \frac{[A]^{3/2}_m}{[A]^{3/2}_f} \times \frac{[p_0]_m}{[p_0]_f} \times \frac{[\rho]_f}{[\rho]_m}$$

If the atmospheric pressure and density are the same in full-and model-scale, this gives: $\dfrac{[V_0]_m}{[V_0]_f} = \dfrac{[L]^3_m}{[L]^3_f} \times \dfrac{[\bar{u}]^2_f}{[\bar{u}]^2_m}$ where [L] is a characteristic length scale

Thus similarity can be maintained by increasing the internal volume in the wind tunnel test by the square of the full scale/model velocity ratio. It is interesting and significant that the same scaling relationship has been arrived at by Tryggvason (28) in considering the modelling of inflatable structures. In practice, it is not difficult to provide additional volume beneath the wind tunnel floor to provide the distorted internal volume(28).

## 6. CONCLUSIONS

A combination of theoretical, numerical simulation and boundary layer wind tunnel techniques have been used to investigate internal pressures induced by wind, allowing the following conclusions to be drawn:

(i) Mean and root-mean-square fluctuating internal pressure coefficients increase monotonically with increasing windward/leeward open area ratio, in the former case, in good agreement with a theory based on turbulent flow and mass continuity.

(ii) For the case of a single windward opening, wind tunnel measurements and computer simulated data showed resonance effects on the fluctuating internal pressures. The resonant frequency increases and damping decreases with increasing open area.

(iii) Reasonable agreement between the simulated and measured spectra was achieved when an orifice coefficient of 0.15 was used for the highly unsteady and reversing flow in and out of the orifice.

(iv) Because the resonant frequencies are high in comparison with those of the external wind velocity and stagnation pressures, the resonant effects do not contribute greatly to the total r.m.s. pressure fluctuations.

(v) Inertia effects may, however, be significant if a sudden change in external pressure, such as that due to a window failure, occurs for large openings.

(vi) The effects of not correctly satisfying the scaling requirements for fluctuating internal pressures by not wind tunnel testing at full scale wind velocities, are probably small in most cases. However, it appears that the effect of higher wind velocities can be simulated by distorting the internal volume by a factor equal to the square of the velocity ratio.

ACKNOWLEDGEMENTS

The author would like to acknowledge the considerable contribution of Joe Munarin, Gordon McNealy and Ross Best towards the work described herein. Discussions with Bjarni Tryggvason also proved extremely useful. The work was sponsored by the Australian Housing Research Council.

REFERENCES:

(1) Walker, G.R., "Report on Cyclone 'Tracy' - Effect on Buildings" Australian Department of Housing and Construction (1965).

(2) Euteneuer, G.A., "Einfluss des Windeinfalls auf Innendruck und Zugluft-Erscheinung in teilweise offenen Bauwerken". Der Bauingenieur 46: 355-360(1971)

(3) Van Koten, H., "The Wind Pressures on Windows" Symposium on Full Scale Measurements of Wind Effects London, Ontario (1974).

(4) Newberry, C.W. and Eaton, J.J., "Wind Loading Handbook" Building Research Establishment (U.K.) (1974).

(5) Liu, H., "Wind Pressure inside Buildings" 2nd U.S. National Conference on Wind Engineering Research Fort Collins, Colorado (1975).

(6) S.A.A. "Loading Code. Part 2 - Wind Forces" A.S. 1170 Part 2 Standards Association of Australia (1975).

(7) Euteneuer, G.A., "Druckansteig im Inneren von Gebaüden bei Windeinfall" Der Bauingenieur 45: 214-216 (1970).

(8) Vickery, B.J., "Internal Pressures", Section 10.8 in The Structural and Environmental Effects of Wind on Buildings and Structures Course Notes, Monash University (1975).

(9) Liu, H., "Building Code Requirements on Internal Pressure", 3rd U.S. National Conference on Wind Engineering Research Gainesville, Florida (1978).

(10) Jancauskas, E.D. and Sharp, D.B., "Wind Loading on the Roof of a Low-Rise House" 6th Australasian Hydraulics and Fluid Mechanics Conference Adelaide(1977)

(11) Kramer, C., Gerhardt, H.J. and Scherer, S., "Wind Pressure on Block-type Buildings" 3rd Colloquium on Industrial Aerodynamics Aachen (1978).

(12) Holmes, J.D., "Mean and Fluctuating Internal Pressures Induced by Wind" James Cook University of North Queensland. Wind Engineering Report 5/78 (1978).

(13) Rayleigh, Lord "Theory of Sound - Volume 2" Macmillan 1896. Reprinted by Dover Publications (1945).

(14) Malecki, I., Physical Foundations of Technical Acoustics Pergamon Press (1969).

(15) Holmes, J.D., "Design and Performance of a Wind Tunnel for Modelling the Atmospheric Boundary Layer in Strong Winds" James Cook University of North Queensland. Wind Engineering Report 2/77 (1977).

(16) Holmes, J.D. and Best, R.J., "Wind Tunnel Measurements of Mean Pressures on House Models and Comparison with Full Scale Data" 6th Australasian Hydraulics and Fluid Mechanics Conference Adelaide (1977).

(17) Holmes, J.D. and Best, R.J., "Wind Pressures on an Isolated High-Set House" James Cook University. Wind Engineering Report 1/78 (1978).

(18) Holmes, J.D. and Best, R.J., "Further Measurements on Wind Tunnel Models of the Aylesbury Experimental House" James Cook University of North Queensland. Wind Engineering Report 4/78 (1978).

(19) Best, R.J. and Holmes, J.D., "Model Study of Wind Pressures on an Isolated Single-Storey House" James Cook University. Wind Engineering Report 3/78 (1978).

(20) E.S.D.U. "Characteristics of Atmospheric Turbulence Near the Ground - Part II: Single Point Data for Strong Winds (neutral atmosphere)" Engineering Sciences Data Unit (U.K.) Data Item 74031 (1974).

(21) Munarin, J., "Wind Tunnel Measurements of Internal Pressures in a Two Storey House" B.E. Thesis Department of Civil and Systems Engineering, James Cook University (1978).

(22) Holmes, J.D., "Computer Simulation of Multiple Correlated Wind Records Using the Inverse Fast Fourier Transform" Civ. Engg. Trans. Inst. Eng. Austr. CE20: 67-74 (1978).

(23) Biggs, J.M., "Introduction to Structural Dynamics" McGraw-Hill (1964).

(24) Bearman, P.W., "An Investigation of the Forces on Flat Plates in Turbulent Flow" N.P.L. Aero. Report 1296 (1969).

(25) Bearman, P.W., "Some Measurements of the Distortion of Turbulence Approaching a Two-Dimensional Body" A.G.A.R.D Conference on Turbulent Shear Flows (1971).

(26) Holmes, J.D., "Pressure Fluctuations on a Large Building and Along-Wind Structural Loading" J. Indust. Aero. 1: 249-278 (1976).

(27) Pankhurst, R.C. and Holder, D.W., Wind Tunnel Techniques Pitman, London (1952).

(28) Tryggvason, B.V. "Aeroelastic Modelling of Pneumatic and Tensioned Fabric Structures" 5th International Conference on Wind Engineering Ft. Collins(1979).